NANO LETTERS

Letter

pubs.acs.org/NanoLett

Probing Optical Transitions in Individual Carbon Nanotubes Using Polarized Photocurrent Spectroscopy

Maria Barkelid,*[,†] Gary A. Steele,[‡] and Val Zwiller[†]

[†]Quantum Transport Group, Kavli Institute of Nanoscience, Delft University of Technology, Delft, The Netherlands

[‡]Molecular Electronics and Devices, Kavli Institute of Nanoscience, Delft University of Technology, Delft, The Netherlands

Supporting Information

ABSTRACT: Carbon nanotubes show vast potential to be used as building blocks for photodetection applications. However, measurements of fundamental optical properties, such as the absorption coefficient and the dielectric constant, have not been accurately performed on a single pristine carbon nanotube. Here we show polarization-dependent photocurrent spectroscopy, performed on a p−n junction in a single suspended semiconducting carbon nanotube. We observe an enhanced absorption in the carbon nanotube optical resonances, and an external quantum efficiency of 12.3% and 8.7% was deduced for the E11 and E22 transitions, respectively. By studying the polarization dependence of the photocurrent, a dielectric constant of 3.6 ± 0.2 was experimentally determined for this semiconducting carbon nanotube.

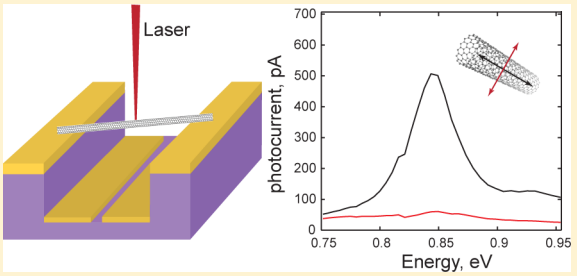

KEYWORDS: *Carbon nanotube, p−n junction, photocurrent spectroscopy, polarization, dielectric constant, quantum efficiency*

Carbon nanotubes show attractive optical[1,2] properties as a direct result of their quasi-one-dimensional geometry. This has triggered an active interest in developing carbon nanotubes for optoelectronic device applications,[3] such as diodes[4,5] and photodetectors.[6] For advanced device design a detailed knowledge about the fundamental physical properties of the system is required. Previous studies have already demonstrated a direct band gap and large exciton binding energies in carbon nanotubes.[1] Optical resonances in the joint density of states arise as a direct result of the quantized nature of the k-vector in the circumferential direction of the carbon nanotube. Optical absorption has been previously reported for carbon nanotube films,[7−9] nanotubes in solution,[10] and nanotubes confined in zeolite channels,[11] but quantitative measurement of the absorption coefficient for an individual carbon nanotube without environmental influence has not been reported.

Here we show polarization dependence of photocurrent spectroscopy measurements[12,13] on a single semiconducting carbon nanotube p−n junction. Using polarization, resonances of the same or of different indices can be separately addressed.[7,8,14−16] We use this polarization dependence to probe the E11 and E22 optical transitions[17] and study the enhanced absorption in these optical resonances. We obtain a quantitative number for the quantum efficiency and attribute this to a lower limit for the absorption coefficient in this semiconducting carbon nanotube, something which has not been previously reported for a single clean nanotube. In addition, we obtain a value for the dielectric constant through experimental measurements. This property of a carbon nanotube has been theoretically predicted and is commonly used as a fitting parameter; however, to the authors' best knowledge no experimental measurement has been reported for this parameter on a single nanotube level.

For this work we fabricated electrically contacted individual semiconducting carbon nanotubes. The nanotubes were synthesized using chemical vapor deposition[18] on a prefabricated device structure.[19] Growing the nanotubes in the final fabrication step ensured a pristine system for the photocurrent study. Figure 1a illustrates the carbon nanotube bridging a 4 μm wide trench in between two W/Pt contacts. In the bottom of the 800 nm deep trench two buried W/Pt trench gates were defined, separated by 250 nm. More information about the device fabrication can be found in the Methods section. The local gate structure was used to engineer the potential landscape of the carbon nanotube.[4,19,20] The nanotube device is subject to electrostatic doping, accomplished by applying voltage to the trench gates. Voltage of opposite polarity applied to the two trench gates realizes a p−n junction in the carbon nanotube. Figure 1b shows a schematic of the electrostatic potential for the p−n junction.

The p−n junction was characterized at room temperature, under vacuum, using scanning photocurrent microscopy[21−24] (λ = 532 nm, power = 1.45 kW/cm^2). Figure 1c shows a scanning photocurrent image of the carbon nanotube p−n junction (color) superimposed on a reflection image (gray) where the metallic contacts and gate structure are visible. The photocurrent image in Figure 1c provides spatial information

Received: July 27, 2012
Revised: September 28, 2012
Published: October 15, 2012

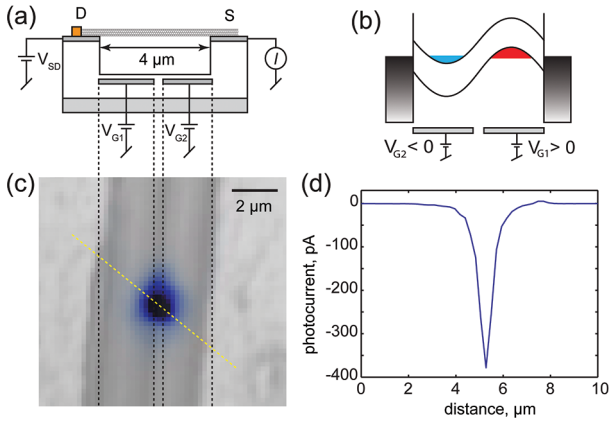

Figure 1. Photocurrent imaging of a suspended carbon nanotube. (a) Device schematic. The nanotube is suspended between two metal contacts, and the device structure contains two trench gates. (b) Schematic of the electrostatic potential of the gate-defined p−n junction. (c) Photocurrent imaging of the p−n junction, determining the location of the maximum electric field to be in the center of the trench. (d) Line profile of the photocurrent along the yellow dashed line in (c) showing the magnitude of the photocurrent signal.

about the electric field in the depletion region. This shows that the photocurrent response indeed originates from the p−n junction which is formed in between the two trench gates. In Figure 1d, the corresponding line profile of the photocurrent image (along the yellow dashed line in Figure 1c) indicates the magnitude of the photocurrent response. The full width at half-maximum of the photocurrent peak measures 660 nm, which is close to our diffraction limited laser spot diameter.

We now position our laser on the p−n junction and study the effect of polarization on the photocurrent response of our nanotube device. When the excitation laser is polarized, two effects are present in the carbon nanotube. One is the depolarization effect, displayed in Figure 2a. The measured polarization dependence of the photocurrent, collected at 1064 nm (0.91 kW/cm^2), demonstrates the polarizability of our carbon nanotube.[25] This effect arises from the one-dimensional geometry of the carbon nanotube. It results in a smaller part of

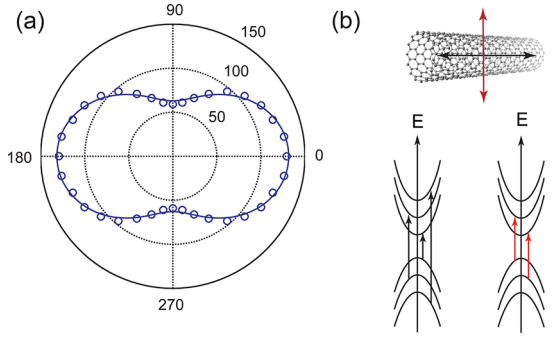

Figure 2. Effect of polarized light on a carbon nanotube. (a) The depolarization effect. Photocurrent measurements were performed at 1064 nm as a function of polarization angle of the incident laser light. The photocurrent is displayed in units of pA. (b) Nanotube selection rules, where light polarized parallel to the nanotube axis probes transitions between subbands of the same index and light polarized perpendicular to the nanotube axis addresses transitions between subbands whose index differ by 1.

the incident electric field coupling in to the carbon nanotube for cross-polarized light.

The second effect that appears for polarized excitation of a carbon nanotube originates from the optical selection rules, schematically illustrated in Figure 2b. Consider the matrix element for an optical transition E_{ij}, as predicted by Ajiki and Ando,[25,26] for light polarized parallel to the nanotube axis optical transitions take place between subbands of the same index ($i = j$), which has the same symmetry for the electron wave function. For light polarized perpendicular to the nanotube axis the angular momentum operator changes the quantum number j by one unit. Thus, the allowed optical transitions occur between subbands whose index differs by 1.

By studying the geometric effect of the polarization anisotropy, we can determine the dielectric constant of this carbon nanotube. In Figure 2a, the energy of the laser is off resonance with any optical transition, and hence the density of states in the nanotube is low. For a low density of states the contribution of the carbon nanotube selection rules to the polarization anisotropy is small, and the dominating contribution comes from the depolarization effect. The recorded photocurrent signal can be used as a direct measure of the electric field in the device. We consider the laser excitation field, applied to the nanotube. The external electric field, E_e, fully penetrates the carbon nanotube when the polarization is aligned along the nanotube axis and is probed using the photocurrent, $I_{parallel}$. For cross-polarized light, a smaller fraction of the electric field is coupling in to the nanotube.[27] The amount of the externally applied electric field that is coupling in to the carbon nanotube (the internal field, E_i) is again probed by the photocurrent, $I_{perpendicular}$. The dielectric constant can now be found using the relation

$$E_i = \frac{2\varepsilon_0}{\varepsilon_{nanotube} + \varepsilon_0} E_e \quad (1)$$

where ε_0 is the dielectric constant of the environment (in our case vacuum, giving $\varepsilon_0 = 1$) and $\varepsilon_{nanotube}$ is the dielectric constant of the carbon nanotube. Within this model we consider the carbon nanotube to be a cylinder of infinite length, with a diameter much smaller than the wavelength of the excitation light.[27] Using the detected photocurrent for parallel and perpendicular polarization, a dielectric constant of 3.6 ± 0.2 is found for this semiconducting carbon nanotube. Theory predicts the dielectric constant of a carbon nanotube to assume a value between 1[28] and 4−5[29] (without taking excitonic effects into account). Used as a fitting parameter, a dielectric constant of for example 2.5[17] has been used for a carbon nanotube. Our experimentally measured value for the dielectric constant falls inside the boundaries of the theoretical predictions. The measurement was reproduced on a second semiconducting carbon nanotube device, and a resulting dielectric constant of 3.4 was found (see Supporting Information).

Next we perform polarization-dependent photocurrent spectroscopy with our laser positioned on the p−n junction using a supercontinuum white light source and a tunable filter. See Methods section for further details. Figure 3 displays the photocurrent spectra for light polarized parallel (black) and perpendicular (red) to the carbon nanotube axis. In Figure 3a, a clear peak for the E11 transition is visible at 0.85 eV. In agreement with the theoretical predictions[25,26] and earlier work,[7,8,14−16] this transition is probed with parallel polarized light and suppressed for perpendicular polarization. In Figure

dx.doi.org/10.1021/nl302789k | Nano Lett. 2012, 12, 5649−5653

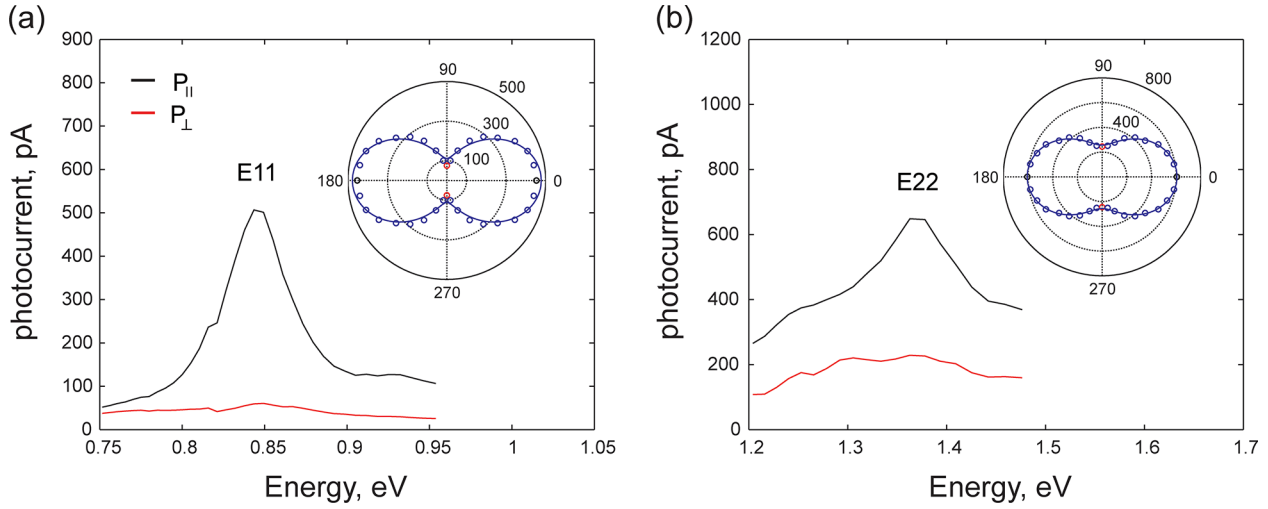

Figure 3. Polarized photocurrent spectroscopy on a p−n junction. (a) Light polarized parallel to the carbon nanotube axis (black) probes the E11 transition at 0.85 eV, and light polarized perpendicular to the carbon nanotube axis (red) suppresses the E11 optical transition. Inset: angular dependence of the photocurrent (units: pA) on the polarization angle of the excitation light. (b) Photocurrent spectroscopy of the E22 optical transition at 1.36 eV. The E22 is probed by parallel polarized light (black) and suppressed for perpendicular polarized light (red). Inset: angular dependence of the photocurrent (units: pA) on the polarization angle for E22.

3b, the E22 transition at 1.36 eV is, according to the same principle, addressed with parallel polarized light and suppressed with perpendicular polarized light. For these parts of the spectrum the spectral output power of the laser is flat with regards to the nanotube features. (See Figure S4 in the Supporting Information.) The insets in Figure 3a,b show the angular dependence of the photocurrent for E11 and E22 as a function of the polarization angle of the incident laser light. A polarization ratio of the carbon nanotube can be defined as $\rho = (I_{\parallel} - I_{\perp})/(I_{\parallel} + I_{\perp})$. The depolarization effect alone gives a polarization ratio of 0.40 ± 0.02. For the E11 transition a polarization ratio of 0.72 ± 0.08 is found, and for E22 the polarization ratio is 0.53 ± 0.05. Calculations reported by Islam et al.[7] show, similarly to our results, a smaller polarizability of E22 compared to E11, as a result of the smaller absorption cross section for the E22 transition. On a resonance the polarizability of the carbon nanotube is a result of both the depolarization effect and the optical selection rules. Knowing the dielectric constant, these two effects could be decoupled. However, variations in the dielectric constant with frequency[29] make it difficult to accurately predict the value of the dielectric constant of a carbon nanotube on an optical resonance. Theoretical calculations have been performed on this frequency variation;[30−32] however, further studies are required on a single nanotube level in the near-infrared part of the spectrum in order to quantify this variation and make an accurate prediction about the decoupling of the two contributions to the polarization anisotropy on an optical resonance. For light polarized perpendicular to the carbon nanotube axis the E12/E21 transition is expected to show up on the low-energy side of the E22 resonance.[15] However, this transition is considerably suppressed as a result of the depolarization effect and therefore not visible in our measurements.

A lower limit of the absorption coefficient for an individual suspended semiconducting carbon nanotube can be determined from the external quantum efficiency of the carbon nanotube device:

$$\mathrm{QE}_{\mathrm{external}} = \frac{\frac{I_{\mathrm{pc}}}{e}}{\frac{P_{\mathrm{laser}}}{E_{\mathrm{ph}}} T_{\mathrm{obj}} \frac{A_{\mathrm{nanotube}}}{A_{\mathrm{laser}}}} \quad (2)$$

where I_{pc} is the measured photocurrent (in A), e is the elementary charge, P_{laser} is the power of the incident laser beam (in W), E_{ph} is the energy of the incident photons, T_{obj} is the transmissivity of the objective, and $A_{\mathrm{nanotube}}/A_{\mathrm{laser}}$ is a normalization with respect to the carbon nanotube surface area exposed to the incident laser beam. The external quantum efficiency is a combination of the absorption coefficient of the carbon nanotube and the internal quantum efficiency of the p−n junction. Hence, this external quantum efficiency provides a lower limit of the absorption coefficient in this suspended semiconducting carbon nanotube. From eq 2 an external quantum efficiency of 0.123 electrons/photons was found for the E11 transition, and a lower limit of the absorption coefficient is 12.3%. Similarly for the E22 transition, the external quantum efficiency is 0.087, and a lower limit for the absorption coefficient is 8.7%. These results agree well with values reported by Freitag et al.[6] where the authors estimate a quantum efficiency of >10% for their single nanotube FET device. For a wavelength off resonance, the extracted lower limit of the absorption coefficient is around 3%, comparable to that measured for graphene samples.[33] This demonstrates the enhanced absorption for a carbon nanotube when the energy of the excitation laser is on resonance with an optical transition. Figure 4 shows the external quantum efficiency, calculated according to eq 2, as a function of incident laser power. The efficiency of the device is higher at lower laser powers for both the E11 and the E22 transition. The decreasing efficiency could be attributed to charge accumulation in the device at higher laser powers.[34] Another possible explanation for the decreasing quantum efficiency could be local heating of the nanotube induced by increased laser power. Heating could increase the charge carrier relaxation rate and hence decrease the internal efficiency of the p−n junction and thereby the external quantum efficiency. The absorption in the E22 is generally

dx.doi.org/10.1021/nl302789k | Nano Lett. 2012, 12, 5649−5653

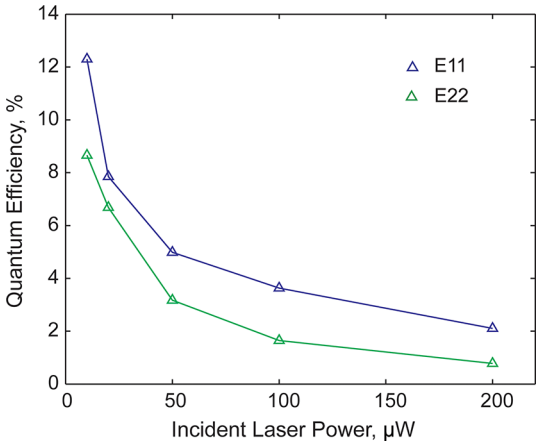

Figure 4. Calculated external quantum efficiency as a function of incident laser power. As the laser power is increased, the quantum efficiency decreases for both the E11 and E22 transition. The lines connecting the measurement points serve as a guide to the eye. This quantum efficiency serves as a lower limit for the absorption coefficient in the carbon nanotube device.

lower than the absorption in the E11, which is in agreement with previous findings.[7]

In conclusion, polarization-dependent photocurrent spectroscopy has been performed on a carbon nanotube p−n junction. The E11 and E22 optical transitions could be readily probed in parallel polarization and is suppressed for perpendicularly polarized light. By studying the polarization anisotropy off resonance a dielectric constant of 3.6 ± 0.2 could be extracted from the depolarization effect. An external quantum efficiency of 12.3% and 8.7% were measured for the E11 and E22 optical resonances, respectively, and this states a lower limit for the absorption coefficient for a single semiconducting carbon nanotube. Experimentally verified values for these physical properties of a carbon nanotube open up possibilities for development of future optoelectronic carbon nanotube devices, such as photodetectors and phototransistors, operating in the near-infrared part of the spectrum. A carbon nanotube with a suitable optical resonance could be used for designing photodetectors for telecommunication applications. In addition, this work also demonstrates polarization-dependent photocurrent spectroscopy as a tool for probing selected optical transitions in individual carbon nanotubes.

Methods. The carbon nanotube device was fabricated starting from a piece of Si wafer covered with 285 nm thermal SiO_2. Trench gates were patterned using electron beam lithography followed by evaporation of 5 nm W and 25 nm Pt. The gates were 2 μm wide each and separated by 250 nm.

Next, 1 μm of SiO_2 was deposited using PECVD, and the oxide was thereafter etched away above the gates, creating an 800 nm deep and 4 μm wide trench. This left an insulating layer of SiO_2 on top of the gates. The source and drain contacts were defined on top of the SiO_2 mesas with electron beam lithography and metal evaporation (5 nm W and 25 nm Pt).

A catalyst area was patterned with electron beam lithography on top of the metal contact and the catalyst solution was drop-coated on to the sample and lifted off in hot acetone. This left a well-defined area of silica nanoparticles and FeMo catalysts for the carbon nanotube synthesis.

Finally, the carbon nanotubes were grown in a CVD oven at 900 °C under CH_4 and H_2 flow. After starting growing from the defined catalyst area the carbon nanotubes extended across the trench and made an electrical contact between the source and drain electrode.

The suspended carbon nanotube devices were characterized by scanning the laser beam across a defined area of the sample by means of two computer-controlled scanning mirrors. The laser was focused onto the sample with an IR-coated objective with a numerical aperture of 0.8.

In photocurrent imaging the reflected light from the sample structure was collected by a photodiode, generating a reflection image of the sample. Simultaneously, the current through the carbon nanotube was measured for every laser coordinate, generating a photocurrent image. The reflection and photocurrent images were superimposed creating an image of spatial photocurrent response in relation to the metallic device structure.

Basic characterization was performed with a 532 nm laser. The E11 and E22 transitions were probed using a Fianium supercontinuum white light source, pulsed at 20 MHz, and an acousto-optic tunable filter (AOTF) which generated a collimated laser beam for wavelengths between 650 and 1100 nm with 5 nm bandwidth (crystal 1) and between 1100 and 2000 nm with 7 nm bandwidth (crystal 2).

■ ASSOCIATED CONTENT

Ⓢ Supporting Information

Additional device characterization as well as complementary data for the carbon nanotube device measured in a n−p doping configuration and measurements of the dielectric constant on a second carbon nanotube device. This material is available free of charge via the Internet at http://pubs.acs.org.

■ AUTHOR INFORMATION

Corresponding Author

*E-mail k.m.barkelid@tudelft.nl.

Author Contributions

The manuscript has been prepared through contributions of all authors.

Notes

The authors declare no competing financial interest.

■ ACKNOWLEDGMENTS

This work was supported through a FOM Project Ruimte.

■ REFERENCES

(1) Dresselhaus, M. S.; Dresselhaus, G.; Saito, R.; Jorio, A. Exciton Photophysics of Carbon Nanotubes. *Annu. Rev. Phys. Chem.* **2007**, *58*, 719−747.

(2) Jorio, A.; Saito, R.; Hertel, T.; Weisman, R. B.; Dresselhaus, G.; Dresselhaus, M. S. Carbon Nanotube Photophysics. *Mater. Res. Soc. Bull.* **2004**, *29*, 276−280.

(3) Avouris, P.; Freitag, M.; Perebeinos, V. Carbon-Nanotube Photonics and Optoelectronics. *Nat. Photonics* **2008**, *2*, 341−350.

(4) Lee, J. U.; Gipp, P. P.; Heller, C. M. Carbon Nanotube p-n Junction Diodes. *Appl. Phys. Lett.* **2004**, *85*, 145−147.

(5) Mueller, T.; Kinoshita, M.; Steiner, M.; Perebeinos, V.; Bol, A. A.; Farmer, D. B.; Avouris, P. Efficient Narrow-Band Light Emission From a Single Carbon Nanotube p-n Diodes. *Nat. Nanotechnol.* **2010**, *5*, 27−31.

(6) Freitag, M.; Martin, Y.; Misewich, J. A.; Martel, R.; Avouris, P. H. Photoconductivity of Single Carbon Nanotubes. *Nano Lett.* **2003**, *3*, 1067−1071.

(7) Islam, M. F.; Milkie, D. E.; Kane, C. L.; Yodh, A. G.; Kikkawa, J. M. Direct Measurement of the Polarized Optical Absorption Cross

Section of Single-Wall Carbon Nanotubes. *Phys. Rev. Lett.* **2004**, *93*, 037404.
(8) Murakami, Y.; Einarsson, E.; Edamura, T.; Maruyama, S. Polarization Dependence of the Optical Absorption of Single-Walled Carbon Nanotubes. *Phys. Rev. Lett.* **2005**, *94*, 087402.
(9) Ichida, M.; Mizuno, S.; Tani, Y.; Saito, Y.; Nakamura, A. Exciton Effects of Optical Transitions in Single-Wall Carbon Nanotubes. *J. Phys. Soc. Jpn.* **1999**, *68*, 3131−3133.
(10) Jeong, S. H.; Kim, K. K.; Jeong, S. J.; An, K. H.; Lee, S. H.; Lee, Y. H. Optical Absorption Spectroscopy For Determining Carbon Nanotube Concentration in Solution. *Synth. Met.* **2007**, *157*, 570−574.
(11) Li, Z. M.; Tang, Z. K.; Liu, H. J.; Wang, N.; Chan, C. T.; Saito, R.; Okada, S.; Li, G. D.; Chen, J. S.; Nagasawa, N.; et al. Polarized Absorption Spectra of Single-Walled 4 Å Carbon Nanotubes Aligned in Channels of an $AlPO_4$-5 Single Crystal. *Phys. Rev. Lett.* **2001**, *87*, 127401.
(12) Lee, J. U.; Codella, P. J.; Pietrykowski, M. Direct Probe of Excitonic and Continuum Transitions in the Photocurrent Spectroscopy of Individual Carbon Nanotube p-n Diodes. *Appl. Phys. Lett.* **2007**, *90*, 053103.
(13) Malapanis, A.; Jones, D. A.; Comfort, E.; Lee, J. U. Measuring Carbon Nanotube Band Gaps Through Leakage Current and Excitonic Transitions of Nanotube Diodes. *Nano Lett.* **2011**, *11*, 1946−1951.
(14) Leonard, F. *The Physics of Carbon Nanotube Devices*; William Andrew Inc.: Norwich, 2009; pp 201−205.
(15) Lefebvre, J.; Finnie, P. Polarized Photoluminescence Excitation Spectroscopy of Single-Walled Carbon Nanotubes. *Phys. Rev. Lett.* **2007**, *98*, 167406.
(16) Miyauchi, Y.; Oba, M.; Maruyama, S. Cross-Polarized Optical Absorption of Single-Walled Nanotubes by Polarized Photoluminescence Excitation Spectroscopy. *Phys. Rev. B* **2006**, *74*, 205440.
(17) Wang, F.; Dukovic, G.; Brus, L. E.; Heinz, T. F. The Optical Resonances in Carbon Nanotubes Arise from Excitons. *Science* **2005**, *308*, 838−841.
(18) Kong, J.; Soh, H. T.; Cassell, A. M.; Quate, C. F.; Dai, H. Synthesis of Individual Single-Walled Carbon Nanotubes on Patterned Silicon Wafers. *Nature* **1998**, *395*, 878−881.
(19) Steele, G. A.; Gotz, G.; Kouwenhoven, L. P. Tunable Few-Electron Double Quantum Dots and Klein Tunneling in Ultraclean Carbon Nanotubes. *Nat. Nanotechnol.* **2009**, *4*, 363−367.
(20) Bosnick, K.; Gabor, N.; McEuen, P. Transport in Carbon Nanotube p-i-n Diodes. *Appl. Phys. Lett.* **2006**, *89*, 163121.
(21) Balasubramanian, K.; Burghard, M.; Kern, K.; Scolari, M.; Mews, A. Photocurrent Imaging of Charge Transport Barriers in Carbon Nanotube Devices. *Nano Lett.* **2005**, *5*, 507−510.
(22) Ahn, Y. H.; Tsen, A. W.; Kim, B.; Park, Y. W.; Park, J. Photocurrent Imaging of p-n Junctions in Ambipolar Carbon Nanotube Transistors. *Nano Lett.* **2007**, *7*, 3320−3323.
(23) Buchs, G.; Barkelid, M.; Bagiante, S.; Steele, G. A.; Zwiller, V. Imaging the Formation of a p-n Junction in a Suspended Carbon Nanotube With Scanning Photocurrent Microscopy. *J. Appl. Phys.* **2011**, *110*, 074308.
(24) Freitag, M.; Tsang, J. C.; Bol, A.; Yuan, D.; Liu, J.; Avouris, P. Imaging of the Schottky Barriers and Charge Depletion in Carbon Nanotube Transistors. *Nano Lett.* **2007**, *7*, 2037−2042.
(25) Ajiki, H.; Ando, T. Aharonov-Bohm Effect in Carbon Nanotubes. *Physica B* **1994**, *201*, 349−352.
(26) Ando, T. Excitons in Carbon Nanotubes. *Jpn. J. Appl. Phys.* **1997**, *66*, 1066−1073.
(27) Wang, J.; Gudiksen, M. S.; Duan, X.; Cui, Y.; Lieber, C. M. Highly Polarized Photoluminescence and Photodetection From Single Indium Phosphide Nanowires. *Science* **2001**, *293*, 1455−1457.
(28) Léonard, F.; Tersoff, J. Dielectric Response of Semiconducting Carbon Nanotubes. *Appl. Phys. Lett.* **2002**, *81*, 4835−4837.
(29) Uryu, S.; Ando, T. Exciton Absorption of Perpendicular Polarized Light in Carbon Nanotubes. *Phys. Rev. B* **2006**, *74*, 155411.
(30) Garcia-Vidal, F. J.; Pitarke, J. M.; Pendry, J. B. Effective Medium Theory of the Optical Properties of Aligned Carbon Nanotubes. *Phys. Rev. Lett.* **1997**, *78*, 4289−4292.
(31) Pichler, T.; Knupfer, M.; Golden, M. S.; Fink, J. Localized and Delocalized Electronic States in Single-Wall Carbon Nanotubes. *Phys. Rev. Lett.* **1998**, *80*, 4729−4732.
(32) Wu, X.; Pan, L.; Li, H.; Fan, X.; Ng, T. Y.; Xu, D. Optical Properties of Aligned Carbon Nanotubes. *Phys. Rev. B* **2003**, *68*, 193401.
(33) Bonaccorso, F.; Sun, Z.; Hasan, T.; Ferrari, A. C. Graphene Photonics and Optoelectronics. *Nat. Photonics* **2010**, *4*, 611−622.
(34) Kittel, C. *Introduction to Solid State Physics*; John Wiley & Sons, Inc.: New York, 1966; p 552.